Preliminary Materials Mapping in the Park City Region for the Utah USGS-EPA Imaging Spectroscopy Project using both high and low altitude AVIRIS data

Barnaby W. Rockwell, Roger N. Clark, K. Eric Livo,
Robert R. McDougal, Raymond F. Kokaly, and J. Sam Vance

United States Geological Survey
Denver, Colorado
http://speclab.cr.usgs.gov

1. INTRODUCTION

This paper presents the preliminary results of AVIRIS-based materials mapping in the region surrounding Park City, Utah. This work was performed as a part of the USGS-EPA Utah Abandoned Mine Lands (AML) Imaging Spectroscopy Project, in which spectroscopic imaging and analysis is being employed for watershed evaluation in areas of past and present mining activity. The objective of the project is to map surface mineralogy and vegetation type/vigor in five major mining districts in Utah with the purpose of identifying sources and environmental effects of acid drainage. The Park City district, located approximately 35 km ESE of Salt Lake City, Utah, is of particular interest because Park City will be the site of the winter Olympics in 2002.

The preliminary results presented here will be field checked during the summer of 1999. It is anticipated that these results will aid the other researchers in private industry and academia who are participating in the USEPA-sponsored Utah AML project. The results and detailed information regarding AVIRIS data calibration will be available online at the USGS Spectroscopy Laboratory web site.

2. GEOLOGIC SETTING, ORE DEPOSITS, AND ALTERATION

The Park City mining district is situated near the intersection of the north-trending Wasatch Range and the west-trending Uinta arch. Intermediate-composition Tertiary stocks have intruded a 3,000 meter thick sequence of Precambrian, Paleozoic and Mesozoic sedimentary rocks. These stocks (see Figure 1) intruded along an east-trending linear zone aligned with the Bingham Canyon deposit in the Oquirrh Mountains 50 km to the west. The Tertiary stocks are porphyries with phenocrysts of plagioclase, hornblende, biotite and pyroxene, with lithologies ranging from quartz granodiorites to monzonites and latites (Erickson et al, 1968). The sedimentary formations include limestone, dolomite, sandstone, siltstone, and argillite, and were folded and thrust faulted during the Cretaceous Sevier orogeny. The district is centered on one of these folds, the north-trending Park City anticline.

The Oligocene Keetly volcanic sequence overlies the folded sedimentary rocks in the eastern part of the study area near the Jordanelle Reservoir (see Figure 1). Stocks in the Park City district may represent source vents for these younger volcanic rocks. Erosion has removed the Keetly volcanic rocks from the main part of the district. Tertiary high-angle faults cut the sedimentary and volcanic rocks and form a ENE-trending zone along which the ore deposits are localized. These northwards-dipping fault zones are often characterized by breccias, slickensides, and abundant iron oxides and hydroxides.

Park City is an epigenetic polymetallic deposit formed at high temperatures (200° - 300° C) during and immediately after intrusion of the stocks at about 33-36 Ma (Bromfield, 1989). The ore occurs as fissure veins in both igneous and sedimentary rocks and as stratabound, manto-type replacement deposits in favorable carbonate units along fault fissures which cut the porphyritic stocks. Although the ore deposits are spatially associated with the intrusions, most mineralization is believed to postdate the intrusive events. Metal production data for the Park City district includes (through 1982): gold (1.5 million ounces), silver (253 million ounces), copper (129 million pounds), lead (2.7 billion pounds), and zinc (1.5 billion pounds). The bonanza-grade oxidized lead-silver ores

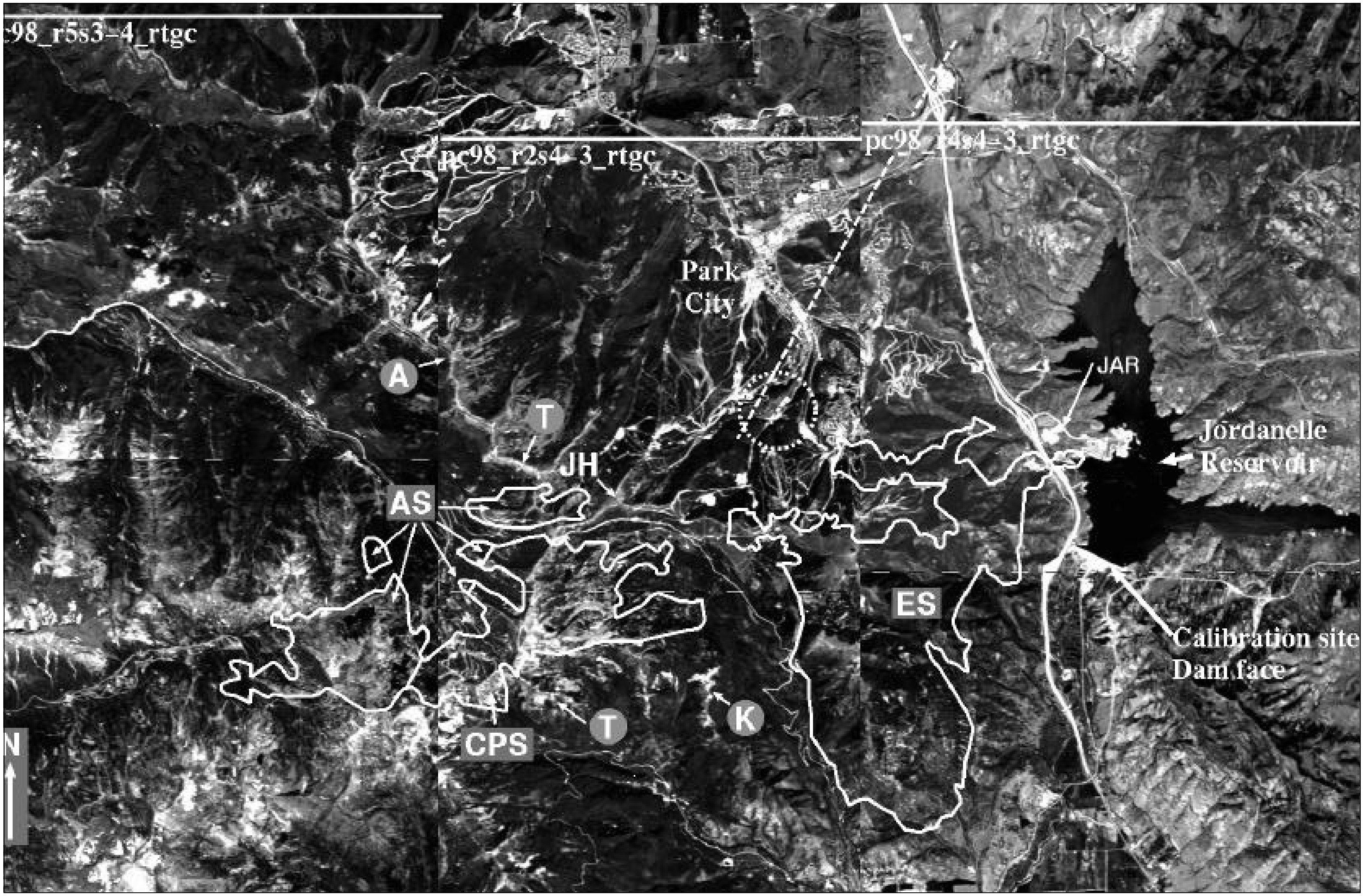

Figure 1. Index image map of the Park City region, Utah. Image is a mosaic of high altitude AVIRIS quicklooks. Heavy horizontal white lines indicate edges of 1024-line AVIRIS image blocks processed by the USGS (scene nomenclature is also annotated). White hashed circle indicates waste rock piles in Empire Canyon shown in mineral maps on Plates 1 and 2. Heavy dashed line indicates approximate centerline of low altitude AVIRIS flightline along the Silver Creek drainage. **JAR** = jarosite. **K** = kaolinite**.** **T** = talc/smectite. **A** = alunite and pyrophyllite. **AS** = Alta stock. **CPS** = Clayton Peak stock. **ES** = eastern stocks (including Ontario, Mayflower, Valeo, Flagstaff, and Pine Creek stocks). **JH** = Jupiter Hill. Some data from Bryant, 1992.

discovered by early prospectors (and long ago mined out) contained cerussite, anglesite, iron oxides, argentite, azurite, malachite and chrysocolla (Koschmann et al, 1968). The main sulfide ore minerals are galena, sphalerite and pyrite, with tetrahedrite-tennantite, chalcopyrite, enargite, and other Pb/Cu/Sb sulfosalts. Principal gangue minerals are quartz and calcite, with less abundant hematite, chlorite, rhodochrosite and anhydrite.

Large exposures of bleached, iron-stained gossans are not abundant in the district. Contact metamorphism near the Clayton Peak Stock (see Figure 1) has created marbleized limestones, and hornfels/argillite from shales. These rocks crop out along the east-trending ridge near Jupiter Hill (see Figure 1) (Bromfield, 1989). Also present in altered carbonate units near the stocks are specular hematite, epidote, and calc-silicate minerals (skarns).

Propylitic alteration of the stocks is present in the eastern part of the district in the hills to the west of the Jordanelle Reservoir (see Figure 1). Mild propylitic alteration consists of aggregates of chlorite, iron oxides and calcite after biotite and hornblende. More intense alteration has produced calcite from plagioclase and epidote from both feldspars and mafic minerals. The Clayton Peak and Pine Creek stocks are relatively unaltered. Intense silicification, sericitization and pyritization (QSP alteration), and formation of hydrothermal phlogopitic biotite, is limited to a small area in the eastern part of the district along the strike of the Mayflower/Pearl vein/fault system.

3. AVIRIS DATA CALIBRATION

High altitude AVIRIS imagery was acquired over the Park City region on August 5, 1998, and low altitude imagery was acquired over the Silver Creek drainage on October 12, 1998 (for AVIRIS quicklooks and flight information, see the JPL AVIRIS web site, **ftp://makalu.jpl.nasa.gov** and the USGS web site, **http://speclab.cr.usgs.gov/earth.studies/Utah-1/utah-1.html)**. The high altitude imagery was calibrated to reflectance using the radiative transfer-ground calibration (RTGC) procedure described in Clark et al (1999). For additional discussions, see this reference and the USGS Spectroscopy Lab web site for detailed information regarding the calibration of the Park City AVIRIS imagery (see **http://speclab.cr.usgs.gov/earth.studies/Utah-1/park_city_calibration.html**). As the low altitude imagery did not cover any of the field calibration sites used for this study, the fully calibrated high altitude imagery was used in place of field spectra as “ground truth”. This calibration methodology is discussed in more detail below.

Figure 2 shows average reflectance spectra of calcite and dolomite sampled from the calibrated high altitude Park City AVIRIS cube. Significant artifacts due to atmospheric water, oxygen, and CO_2 are evident. Even though the AVIRIS data were acquired on a relatively clear day, the atmosphere across the Park City region is highly variable due to almost 5,000 feet of vertical relief. The spectrum of dolomite was sampled from an area at a much higher elevation than the calibration site, and consequently, the corrected data show localized CO_2 residual absorptions. Spectra from the USGS reflectance cube were compared with spectra sampled from a cube calibrated using the JPL calibration methodology (Green et al, 1993). The JPL calibration did not exhibit marked improvement over the USGS RTGC calibration in terms of reducing atmospheric absorption effects.

As no field spectra were obtained during the low altitude overflights, and the flightline did not cover either of the two dam face calibration sites used for the high altitude data, RTGC-calibrated high altitude AVIRIS spectra were used in place of field spectra to simulate ground truth for the low altitude image calibration. Pixels of a bright waste rock pile in Empire Canyon (see Figure 1) were sampled from the RTGC-calibrated high altitude AVIRIS cube, averaged, and edited to remove residual atmospheric absorptions. Figure 3 shows the edited high altitude AVIRIS reflectance spectrum as a solid black line. The unedited spectrum is shown in a fine hashed line behind the edited spectrum. The artifacts removed by the editing are apparent. Figure 3 also shows an average ATREM- and path radiance-corrected low altitude AVIRIS spectrum of the waste rock pile (Gao et al, 1990, 1992). This spectrum was divided into the edited high altitude reflectance spectrum to obtain the MULTIPLIER spectrum used to calibrate the low altitude cube.

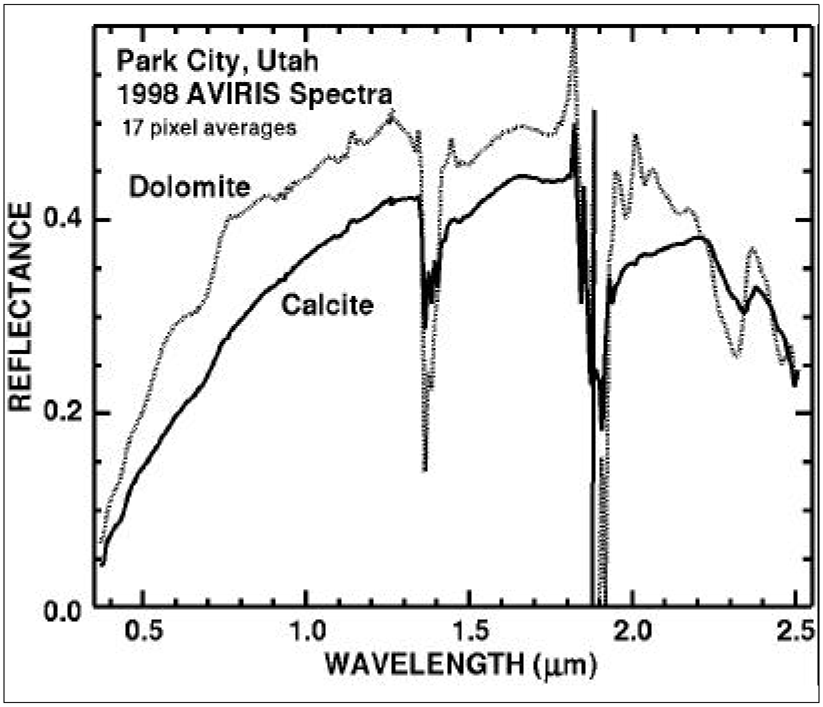

Figure 2. Radiative transfer, ground calibrated (RTGC) AVIRIS spectra from the Park City cube (pc98_r2s4-3.rtgc). Note that residual atmospheric absorptions are much greater in the dolomite spectrum which was sampled from an area several thousand feet above the calibration site.

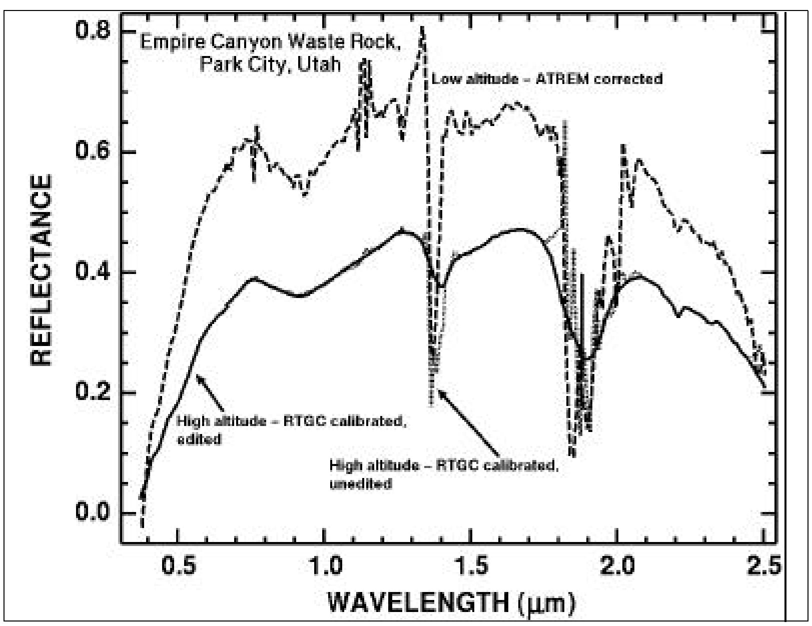

Figure 3. AVIRIS high and low altitude spectra used to calibrate low altitude data to reflectance. Spectra were sampled from a waste rock pile in Empire Canyon.

4. TETRACORDER AUTOMATED IMAGE ANALYSIS

The USGS Tetracorder band shape least-squares spectral mapping algorithm was applied to the calibrated high and low altitude AVIRIS data of the Park City region (Clark et al, 1990, 1991, 1995). Table 1 shows AVIRIS bands which were excluded from the continuum removal and curve fitting analyses due to errors in the radiative transfer atmospheric corrections, other calibration errors, or poor signal-to-noise. The Tetracorder mapping results were sorted relative to curve fit, band depth, and the degree of pixel clustering of each mapped feature. Pixel clustering is a measure of the degree of spatial contiguity of the pixels mapped as a particular class. If the pixels mapped as a particular mineral or vegetation type occur only in a scattered “salt and pepper” pattern, clustering is rated low, whereas if distinct clusters of pixels occur, clustering is rated high. Such a sorting system greatly decreases the time required to evaluate the Tetracorder results.

Plates 1 and 2 show the minerals and mineral mixtures which were mapped with confidence by Tetracorder from the Park City AVIRIS datasets. Although these results have yet to be field checked, each mapped class was verified by extracting spectra from mapped pixels and comparing them with laboratory reference spectra using both visual and continuum removal techniques.

While a vast majority of the mineral classes appear to have mapped correctly in terms of both spectral characteristics and geologic context, several results are in question and require field verification. For example, areas mapped as hectorite and saponite, both trioctahedral members of the smectite clay mineral group, are in question. Hectorite has a deep Mg-OH absorption band centered at 2.305 microns, whereas the Mg-OH feature in

Table 1. AVIRIS channels excluded from Tetracorder Analysis

AVIRIS Channels	Spectral Range (µm)
32-33	0.675-0.664
43	0.760
60-64	0.923-0.961
81-83	1.125-1.144
95-97	1.259-1.255*
106-113	1.345-1.415
152-167	1.803-1.938
173-175	1.999-2.019
179-180	2.059-2.069

*AVIRIS spectrometer overlap

saponite is centered at 2.315 microns. Both minerals also have a subsidiary band at 2.386 microns. Figure 4 shows an average low altitude AVIRIS spectrum of a mineral which mapped as hectorite along with lab spectra of talc, dolomite, and hectorite. It is believed that the mineral mapped in the AVIRIS data is actually talc. Talc is spectrally very similar to hectorite, but is characterized by a shallow band at 2.23 microns and a shoulder at 2.29 microns.

Until field and XRD verification are performed, the minerals mapped as hectorite and saponite have been tentatively re-classified as talc due to spectral similarities and contextual geologic occurrence, which will be discussed below.

Another potentially mis-mapped mineral is halloysite ($Al_2Si_2O_5(OH)_4$), a polymorph with kaolinite, which can be difficult to distinguish from mixtures of kaolinite, muscovite/illite, and/or smectite clays including montmorillonite. When halloysite is mapped in the AVIRIS data, and occurs in close proximity to other phyllosilicates, as mentioned above, its occurrence must be field checked to insure reliability. Such mineral combinations were found to occur in the waste rock piles in Empire Canyon (see Plate 2). However, the mapped minerals show conspicuous layered or zoned patterns in the waste rock pile, not a noisy "salt-and-pepper" pattern, which could indicate that the mixtures are real and not an artifact of the least-squares "binning" process.

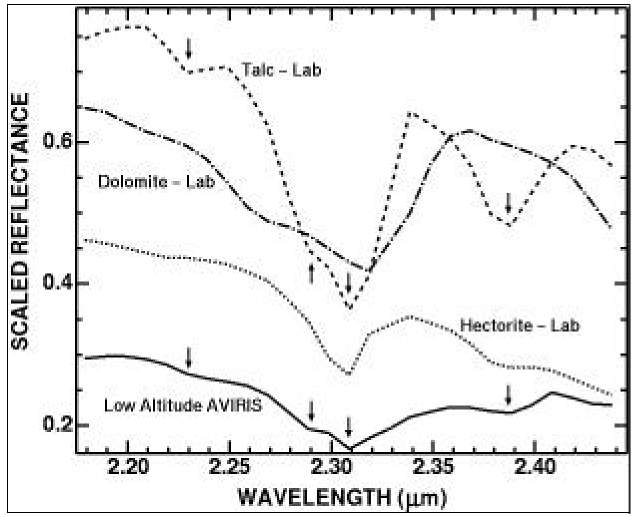

Figure 4. Low altitude AVIRIS spectrum mapped as hectorite with lab spectra for comparison. Arrows indicate features which lead to a re-classification of the mapped mineral as talc.

5. RESULTS AND DISCUSSION

Waste Rock and Mine Sites - Due to extensive vegetation cover, less than 10% of the AVIRIS image block covering Park City (pc98_r2s4-3.rtgc) mapped as minerals or mineral mixtures. Few exposures of jarosite, an iron sulfate mineral noted for generating acidic runoff and thus increased metal mobility, were found in the Park City region. This finding is consistent with other recent USGS studies which found little pyrite in waste rock piles in the Park City district.

Three significant exposures of jarosite were located with the AVIRIS imagery. The first exposure was found in the northwest corner of the waste rock pile in Empire Canyon shown in Plate 1, and was detected by both the high and low altitude AVIRIS data. This exposure is approximately 50 meters across and has been targeted for remediation. The Empire Canyon exposure has a jarosite core rimmed with jarosite plus goethite. Significant amounts of calcite and dolomite were mapped in the same waste rock pile 200 meters to the south (up-gradient) of this jarosite exposure. Such carbonate minerals may serve to buffer acidic solutions emanating from the waste rock pile. The exposure mapped as only one pixel of jarosite and one pixel of goethite on the high altitude data (17.05 m ground resolution). Plates 1 and 2 show that the low altitude AVIRIS data with 1.8 m ground resolution is far superior for mapping small features such as waste rock piles relative to the high altitude data.

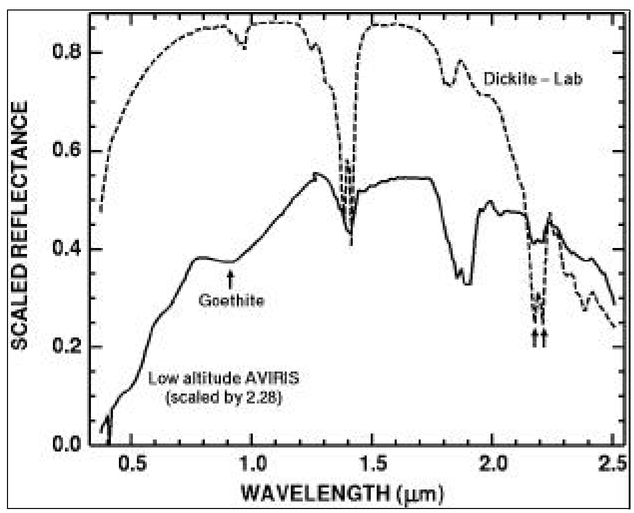

Figure 5. Average low altitude altitude AVIRIS spectrum of mineral mapped as dickite + goethite, with lab reference spectrum of dickite for comparison. Arrows show Al-OH absorption features diagnostic of dickite.

A large exposure of goethite, iron oxides, kaolinite, kaolinite plus muscovite, dickite, and possibly pyrophyllite was mapped with the low altitude AVIRIS data 600 meters to the southwest of the Empire

Canyon jarosite exposure (see Plates 1 and 2). Figure 5 shows an average low altitude AVIRIS spectrum of several pixels from this exposure which mapped as dickite. This concentration of minerals lies near the mouth of the Alliance Tunnel, and would not have been identified with the high altitude data, which indicated only one pixel of goethite. The nearby mouths of the Judge and Anchor drainage tunnels appear to be relatively free of goethite and clay minerals, with more abundant carbonates and muscovite/illite.

A second exposure of jarosite was found on a hillside near the Ontario mine shaft, located 1 km SSE of the waste rock pile in Empire Canyon. This exposure mapped as 5 pixels of jarosite and kaolinite using the high altitude AVIRIS data.

The third important exposure of jarosite was found near the western shore of the Jordanelle Reservoir (AVIRIS image block pc98_r4s4-3.rtgc) and is indicated on Figure 1. This large exposure is approximately 340 m long and 250 m wide and is located near the mouths of McHenry and Glencoe Canyons and Big Dutch Pete Hollow. These canyons are the site of some of the most productive mines in the Park City district, including the Hawkeye/McHenry, Star, Glencoe and Mayflower mines. The Jordanelle exposure is located approximately 0.5 km northeast of the Mayflower mine, which has produced more gold (>900,000 ounces) than any other mine in the district (Bromfield, 1989). The exposure mapped as jarosite, jarosite plus goethite, and goethite. Two pixels of jarosite also mapped at the site of the Star Tunnel in Glencoe Canyon. Figure 6 shows average AVIRIS spectra from the two principal jarosite exposures and the laboratory reference spectrum for comparison. Note the presence of a significant Fe-OH band due to jarosite at 2.26 microns (see arrow) in the high altitude AVIRIS spectrum of the Jordanelle exposure.

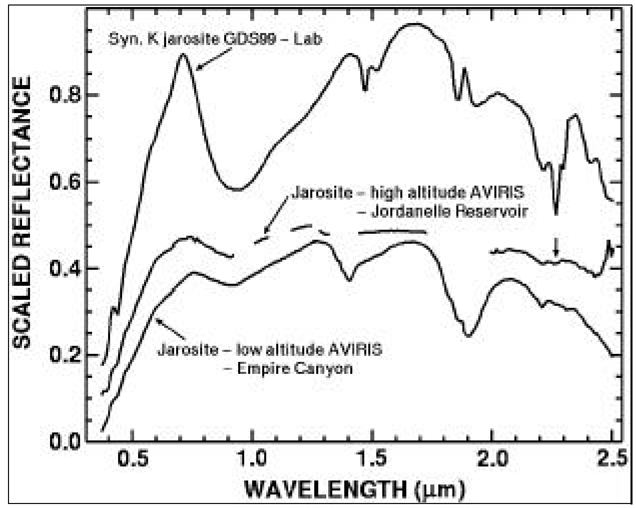

Figure 6. AVIRIS and laboratory spectra of jarosite. Small arrow indicates Fe-OH absorption probably due to jarosite. AVIRIS channels in the atmospheric water bands have been deleted from the high altitude spectrum for clarity.

<u>Natural Alteration and Metamorphic Minerals</u> - Several occurrences of hydrothermal alteration and contact metamorphic minerals were mapped with the high altitude AVIRIS data. Figure 7 shows high altitude AVIRIS spectra of minerals mapped on the summit cone of Jupiter Hill (see Figure 1). This area mapped as intermixed pixels of calcite and epidote. Epidote is spectrally similar to calcite in the 2.0 - 2.5 micron wavelength region of the spectrum, but can be distinguished by a shallow band at 2.25-2.26 microns which is not present in calcite. The summit area of Jupiter Hill is underlain by the Thaynes Limestone, Woodside Shale, and sandstones, mudstones, and limestones of the Ankareh Formation (all Triassic), and is very close to the eastern edge of the Clayton Peak stock. The epidote observed on Jupiter Hill may be an exposure of the contact metamorphic aureole around the Clayton Peak stock, in which carbonate beds were altered to epidote and calc silicate minerals. Iron oxides, hydroxides and small exposures of chlorite were also mapped just below the summit cone. These iron minerals are believed to be associated with intense hydrothermal alteration along an ENE-trending fault zone which traverses this area. This mineralized fault zone has been mined extensively at depth.

Little evidence of the propylitic alteration of the eastern stocks was found. Several pixels of chlorite and calcite were identified in the vicinity of the Star Tunnel near the eastern edge of the Ontario stock. Muscovites possibly related to QSP alteration were also mapped at the Star Tunnel. This area is underlain by the Mayflower-Pearl fault system.

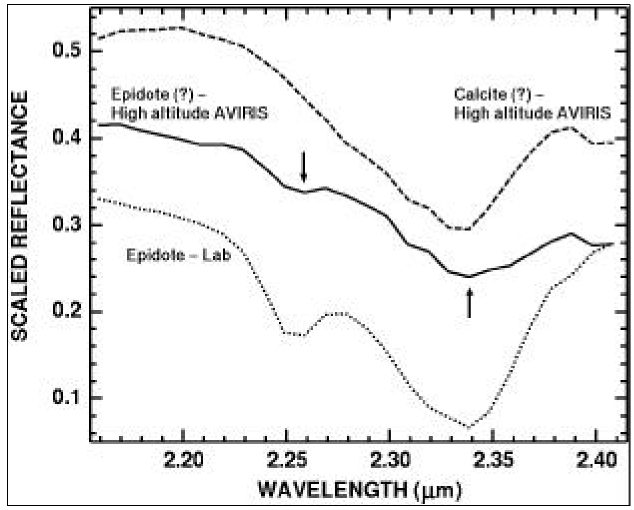

Figure 7. AVIRIS and laboratory spectra of epidote and calcite. Arrows show Fe-OH spectral features in the AVIRIS spectrum of a mineral mapped as epidote near the summit of Jupiter Hill.

Minerals mapped as hectorite and saponite, but re-classified as talc, were found scattered throughout the Park City region (see Figure 4). In Empire Canyon, these minerals occur both as disseminated pixels in soils (upper left of Plate 2) and in concentrated clusters in the waste rock pile. Large exposures of these minerals occur at two undisturbed locations above treeline in close proximity to the Alta and Clayton Peak stocks (see areas marked "T" in Figure 1). The northern of these two locations is underlain by the Thaynes Limestone and Woodside Shale, and the southern exposure is underlain by the Round Valley Limestone and Weber Sandstone (Permian). If the mapped minerals are indeed talc, the exposures may represent evidence of thermal metamorphism of carbonate beds associated with the intrusion of the stocks. Talc is the first new mineral to form as a result of low grade thermal metamorphism of siliceous dolomites (Deer et al, 1966), as represented by the reaction dolomite + quartz -> talc + calcite.

Several undisturbed exposures of minerals commonly associated with argillic hydrothermal alteration were also found, usually in close spatial association with fault zones. Kaolinite was mapped 0.5 km south of a mine shaft in Boulder Basin (see area marked "K" in Figure 1), and near thrust faults to the south of the south end of the Pine Creek stock (area marked "ES" in Figure 1). A small exposure of alunite and pyrophyllite was mapped along the high ridgeline west of Park City (see area marked "A" on Figure 1). Figures 8 and 9 show average high altitude AVIRIS spectra sampled from this exposure. The shallow depth of the diagnostic Al-OH absorption bands indicates that these minerals are present only in very low abundance.

The image block to the west of Park City (pc98_r5s3-4.rtgc), which covers the highlands between Big and Little Cottonwood Canyons and the upper reaches of American Fork Canyon, showed more mineral exposures (about 20%) than the Park City image block. This area is dominated spectrally by calcite and dolomite in the Deseret Limestone, Gardison Limestone, and Fitchville Formation (Upper Devonian/Lower Mississippian), and by muscovite/illite in the Big Cottonwood Formation (Precambrian) and Maxfield Limestone, Ophir Formation, and

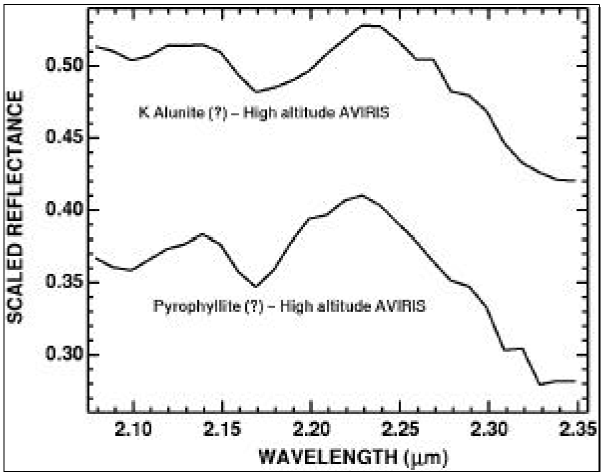

Figure 8. Average high altitude AVIRIS spectra from exposure of argillic alteration on ridge west of Park City (see area marked "A" on Figure 1).

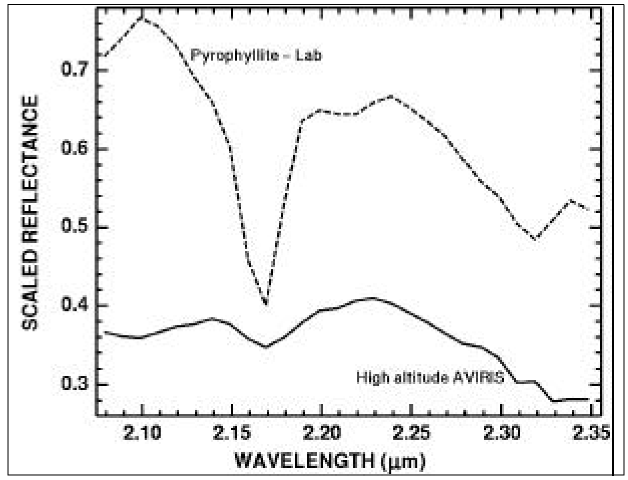

Figure 9. Average high altitude AVIRIS spectrum from Figure 8, with lab spectrum of pyrophyllite for comparison.

Tintic Quartzite (Cambrian) (Bryant, 1992). Some interesting exposures of high temperature alteration minerals such as alunite, dickite, and pyrophyllite were found in the upper reaches of the American Fork Canyon. Several exposures of jarosite were identified in this area as well.

6. CONCLUSIONS

Despite extensive vegetation cover, the AVIRIS imagery proved to be vry useful for mapping both natural and man-made mineral exposures in the Park City region. Few occurrences of jarosite were found, and no evidence was found for downstream movement of metals from mine sites and waste rock piles. However, extensive riparian vegetation cover along streams, and the small spatial scale of the streams in the area, make reliable mineral mapping along the streams nearly impossible with the 1998 AVIRIS imagery. Most of Silver Creek along Empire Canyon was not covered by the low altitude overflight, and was partially occluded by terrain shadow.

The low altitude AVIRIS imagery with 1.8 m ground resolution was far superior for iron species discrimination compared to the high altitude imagery. The substantial terrain relief in the area creates atmospheric variation across the region, resulting in significant artifacts in the calibrated high altitude imagery caused by local variations in atmospheric CO_2, O_2 and water vapor content. Due to the much lower flight altitude (~12,000 feet), such atmospheric artifacts were largely absent from the low altitude AVIRIS imagery.

In general a good correlation exists between the Tetracorder mapping results obtained from the high and low altitude AVIRIS imagery. The mineral and vegetation maps created using the Tetracorder process should serve as useful tools to guide further geochemical and geological sampling programs.

7. REFERENCES

Bromfield, C.S., 1989, Gold deposits in the Park City mining district, Utah, USGS Bull. 1857-C, pp. C14-C26.

Bryant, B., 1992, Geologic and structure maps of the Salt Lake City 1° x 2° quadrangle, Utah and Wyoming, USGS Miscellaneous Investigations Series, Map I-1997, U.S. Government Printing Office, Washington, D.C., Sheet 1 of 3.

Clark, R.N., A.J. Gallagher, and G.A. Swayze, 1990, Material Absorption Band Depth Mapping of Imaging Spectrometer Data Using a Complete Band Shape Least-Squares Fit with Library Reference Spectra, Proceedings of the Second Airborne Visible/Infrared Imaging Spectrometer (AVIRIS) Workshop. JPL Publication 90-54, pp. 176-186.

Clark, R.N., G.A. Swayze, A. Gallagher, N. Gorelick, and F. Kruse, 1991, Mapping with Imaging Spectrometer Data Using the Complete Band Shape Least-Squares Algorithm Simultaneously Fit to Multiple Spectral Features from Multiple Materials, Proceedings of the Third Airborne Visible/Infrared Imaging Spectrometer (AVIRIS) Workshop, JPL Publication 91-28, pp. 2-3.

Clark, R.N. and G.A. Swayze, 1995, Mapping Minerals, Amorphous Materials, Environmental Materials, Vegetation, Water, Ice and Snow, and Other Materials: The USGS Tricorder Algorithm. Summaries of the Fifth Annual JPL Airborne Earth Science Workshop, January 23- 26, Pasadena, CA, R.O. Green, Ed., JPL Publication 95-1, pp. 39-40.

Clark, R.N., G.A. Swayze, T.V.V. King, K.E. Livo, R.F. Kokaly, J.B. Dalton, J.S. Vance, B.W. Rockwell, and R.R. McDougal, 1999, Surface reflectance calibration of terrestrial imaging spectroscopy data: a tutorial using AVIRIS, USGS Open File Report 99- . In press. Available online at:
http://speclab.cr.usgs.gov/PAPERS.calibration.tutorial/calibntA.html

Deer, W.A., R.A. Howie, and J. Zussman, 1966, *An Introduction to the Rock Forming Minerals*, Longman Group, London, p. 228.

Erickson, A.J., W.R. Phillips, and W.J. Garmoe, eds., 1968, Park City District, Utah; *Guidebook to the Geology of Utah*, No. 22, Utah Geological Society, Salt Lake City, Utah, 102 p.

Gao, B.C. and A.F.H. Goetz, 1990, “Column atmospheric water vapor and vegetation liquid water retrievals from airborne imaging spectrometer data”, J. Geophys Res. 95, pp. 3549-3564.

Gao, B.C., K.B. Heidebrecht, and A.F.H. Goetz, 1992, ATmospheric REMoval Program (ATREM) User's Guide, version 1.1, Center for the Study of Earth From Space document, University of Colorado, 24pp.

Green, R.O., J.E. Conel, and D.A. Roberts, 1993, “Estimation of aerosol optical depth, pressure elevation, water vapor and calculation of apparent surface reflectance from radiance measured by the Airborne Visible/Infrared Imaging Spectrometer (AVIRIS) using a radiative transfer code”, SPIE Vol. 1937, Imaging Spectrometry in the Terrestrial Environment, G. Vane, Ed., pp. 2-11.

Koschmann, A.H. and M.H. Bergendahl, 1968, Principal gold-producing districts of the United States, USGS Professional Paper 610, U.S. Government Printing Office, Washington, D.C., pp. 249-250.

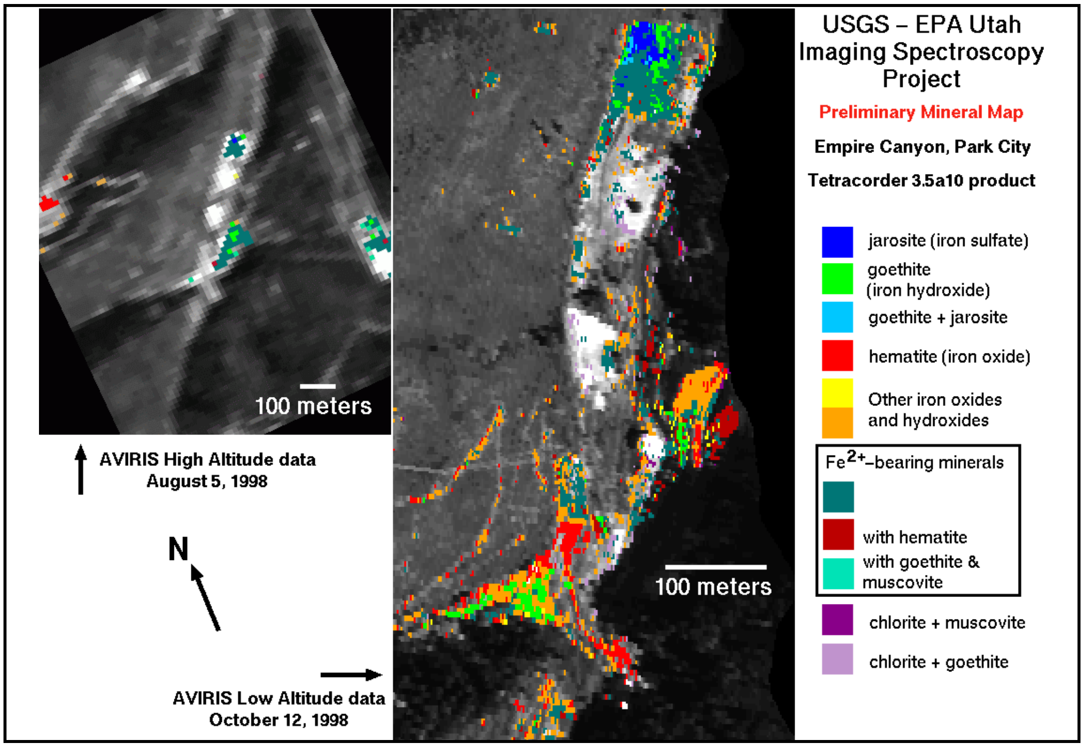

Plate 1. Comparison of Tetracorder mapping results from high and low altitude AVIRIS data in the 0.3 to 1.4 micron spectral region.

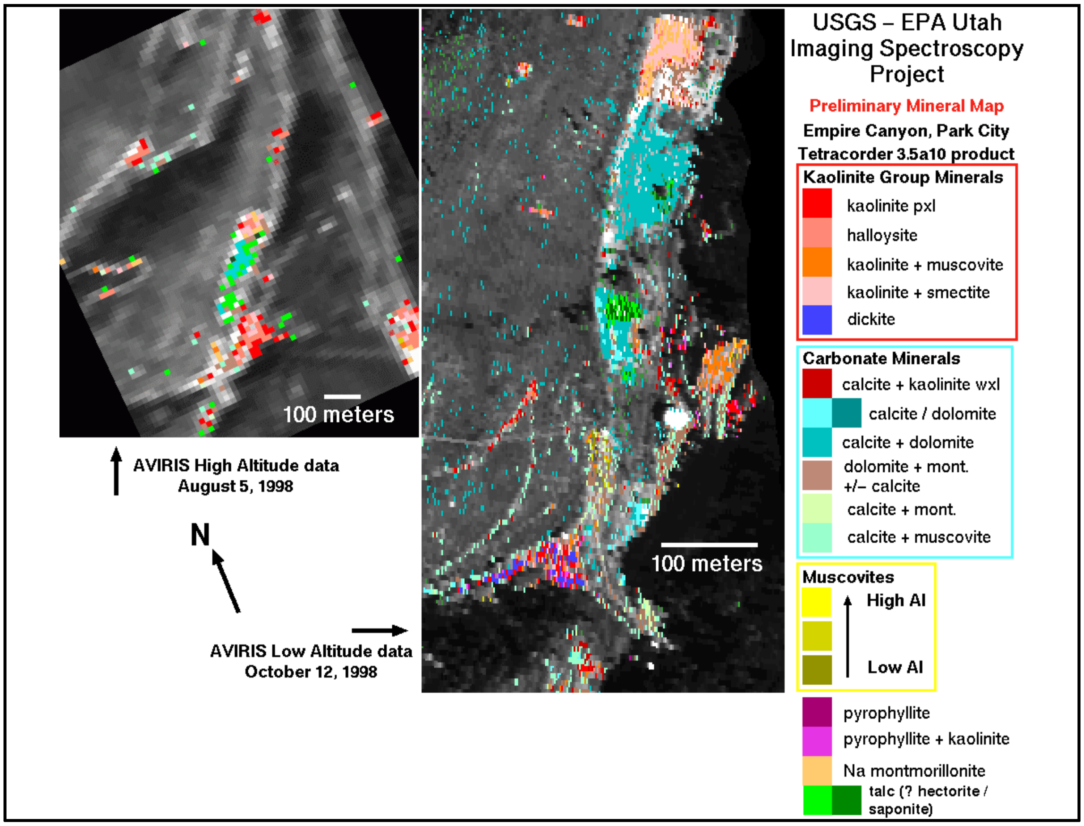

Plate 2. Comparison of Tetracorder mapping results from high and low altitude AVIRIS data in the 2.0 to 2.5 micron spectral region.